JIPB Journal of Integrative Plant Biology

Two hydroxypyruvate reductases encoded by *OsHPR1* and *OsHPR2* are involved in photorespiratory metabolism in rice

Nenghui Ye[1,2], Guozhen Yang[1], Yan Chen[1], Chan Zhang[1], Jianhua Zhang[2,3] and Xinxiang Peng[1]*

[1]State Key Laboratory for Conservation and Utilization of Subtropical Agro-Bioresources, South China Agricultural University, Guangzhou, China, [2]Shenzhen Research Institute, The Chinese University of Hong Kong, Shenzhen, China, [3]State Key Laboratory of Agrobiotechnology, The Chinese University of Hong Kong, Hong Kong, China. *Correspondence: xpeng@scau.edu.cn

Abstract Mutations in the photorespiration pathway display a lethal phenotype in atmospheric air, which can be fully recovered by elevated CO_2. An exception is that mutants of peroxisomal hydroxypyruvate reductase (HPR1) do not have this phenotype, indicating the presence of cytosolic bypass in the photorespiration pathway. In this study, we constructed overexpression of the *OsHPR1* gene and RNA interference plants of Os*HPR1* and *OsHPR2* genes in rice (*Oryza sativa* L. cv. Zhonghua 11). Results from reverse transcription-polymerase chain reaction (RT-PCR), Western blot, and enzyme assays showed that HPR1 activity changed significantly in corresponding transgenic lines without any effect on HPR2 activity, which is the same for HPR2. However, metabolite analysis and the serine glyoxylate aminotransferase (SGAT) activity assay showed that the metabolite flux of photorespiration was disturbed in RNAi lines of both *HPR* genes. Furthermore, HPR1 and HPR2 proteins were located to the peroxisome and cytosol, respectively, by transient expression experiment. Double mutant *hpr1* × *hpr2* was generated by crossing individual mutant of *hpr1* and *hpr2*. The phenotypes of all transgenic lines were determined in ambient air and CO_2-elevated air. The phenotype typical of photorespiration mutants was observed only where activity of both HPR1 and HPR2 were downregulated in the same line. These findings demonstrate that two hydroxypyruvate reductases encoded by *OsHPR1* and *OsHPR2* are involved in photorespiratory metabolism in rice.

Keywords: Photorespiration; hydroxypyruvate reductase; RNA interference; alternative splicing; rice (*Oryza sativa* L.)
Citation: Ye N, Yang G, Chen Y, Zhang C, Zhang J, Peng X (2014) Two hydroxypyruvate reductases encoded by *OsHPR1* and *OsHPR2* are involved in photorespiratory metabolism in rice. **J Integr Plant Biol** XX(XX): XX–XX. doi: 10.1111/jipb.12125
Edited by: Cong-Ming Lu, Institute of Botany, CAS, China
Received Oct. 6, 2013; **Accepted** Oct. 28, 2013
Available online on Oct. 29, 2013 at www.wileyonlinelibrary.com/journal/jipb

Research Article

INTRODUCTION

Photorespiration is one of the most important physiological processes in plants grown under ambient air conditions, which starts from the oxygenation of ribulose1, 5-bisphosphate (RuBP) by RuBP carboxylase-oxygenase (RubisCO), generating one molecule each of 3-phosphoglycerate (3-PGA) and 2-phosphoglycolate (2-PG). Before 2-PG can re-enter the Calvin cycle, at least eight individual enzymatic reactions take place in three different types of organelles, the chloroplasts, peroxisomes, and mitochondria, which comprise the core of photorespiration pathway (Bauwe et al. 2012). Inside the chloroplasts, 2-PG is hydrolyzed by 2-PG phosphatase (PGLP) into glycolate, which transfers to peroxisome and is further oxidized to glyoxylate by glycolate oxidase (GOX). Glyoxylate is then converted into glycine by serine: glyoxylate aminotransferase (SGAT) and glutamate, glyoxylate aminotransferase (GGAT), in the same organelle. Two molecules of glycine from the peroxisome are converted into one molecule of serine by glycine decarboxylase (GDC) and serine hydroxymethyl transferase (SHMT) in mitochondria. Serine moves back to peroxisome where it is converted into hydroxypyruvate (HP) by SGAT, providing substrate for HP reductase (HPR). HPR catalyses HP into glycerate, which is further changed by glycerate 3-kinase (GLYK) into 3-PGA and eventually re-enters the Calvin cycle. Thus, it is now widely assumed that the major function of the photorespiratory pathway is to recycle the toxic compound 2-PG into 3-PGA (Zelitch and Day 1973; Peterhansel et al. 2012; Florian et al. 2013), which is strongly supported by the phenotype of different mutants in photorespiratory pathway (Somerville and Ogren 1980, 1981; Boldt et al. 2005; Bauwe et al. 2010). A distinctive feature of most photorespiratory mutants is that deletion of photorespiratory enzymes typically leads to a strong air sensitivity of the respective mutants, which, however, can be fully recovered by elevated CO_2 conditions in the so-called photorespiration phenotype (Boldt et al. 2005; Voll et al. 2006; Schwarte and Bauwe 2007). However, an exception is that the mutant of peroxisomal hydroxypyruvate reductase (*hpr1*) does not have a typical photorespiration phenotype. Therefore, it was hypothesized that cytosolic hydroxypyruvate reductase (HPR2) could provide a bypass for this mutant, which could also be an efficient compensation for HPR1 in plants under normal conditions (Murray et al. 1989; Kleczkowski et al. 1990; Timm et al. 2008).

The peroxisomal hydroxypyruvate reductase (HPR1; EC 1.1.1.29) has long been known to locate in peroxisome and catalyze the conversion of HP to glycerate. Genomic DNA analysis indicates that the *HPR1* gene has only a single copy in different species (Greenler et al. 1989; Hayashi et al. 1996;

Mano et al. 1997). Like many other peroxisomal enzymes, the expression of *HPR1* gene is also induced by light (Skadsen and Scandalios 1987; Mano et al. 1999; Desai and Hu 2008). Although two different *HPR* cDNAs have been identified in pumpkin, they are produced by alternative splicing from the same *HPR* gene (Mano et al. 1999). However, it was suggested that light regulations on *HPR1* gene expression and alternative splicing were species-specific (Hondred et al. 1987; Sloan et al. 1993; Mano et al. 1997). Without the *hpr1* mutant in pumpkin, it was hard to prove that the cytosolic HPR (HPR2) plays a key role in the bypass flow. Thus, the overflow hypothesis had not been proved for almost 20 years until the identification of *AtHPR2* in *Arabidopsis* (Timm et al. 2008). Although both *hpr1* mutant and *hpr2* mutant resemble wild type (WT) plant, the double mutation of *AtHPR1* and *AtHPR2* causes a distinct air sensitive phenotype. The photosynthetic performance is also dramatically reduced by deleting both the *AtHPR1* and *AtHPR2* gene, indicating the cytosolic HPR of *Arabidopsis* plays an efficient role in compensating for the function of HPR1. To date, only the pumpkin HPR2 and *Arabidopsis* HPR2 have been identified to be the cytosolic HPR. The dissimilar features between these two HPR2 indicate that different species could use multiple mechanisms to deal with the overflow of photorespiration pathway in WT plants. In the present study, we focus on identification of the *OsHPR2* gene and try to interpret the bypass of the photorespiration pathway in rice.

By using the reverse genetic technologies, we constructed a *OsHPR1* overexpression (OE) line and RNA interference (RNAi) line, both of which resemble WT plant in phenotype under atmosphere conditions, although the HPR1 activities had been changed dramatically. Different sizes of HPR1 protein in leaves and roots of OE plants indicated that alternative splicing of the *OsHPR1* gene was inducible by light. According to the sequence of the *AtHPR2* gene, we identified a *HPR2* candidate by Blastn's rice gene bank. Although the RNAi mutant of this candidate gene displayed the same phenotype with WT plant, the combined deletion of it with the *HPR1* gene resulted in a severe air sensitivity, which was recovered by elevated CO_2 condition. The subcellular localization of this HPR2 candidate is in the cytosol, which is different than HPR1, which is located in the peroxisome. Our results strongly suggest that rice NADPH-HPR is encoded by the *OsHPR2* gene rather than by light-induced alternative splicing from the *OsHPR1* gene and that both HPRs are involved in photorespiratory metabolism in rice.

RESULTS

Construction of overexpression and RNAi transgenic lines of rice *OsHPR1* gene

Interestingly, as a model plant, rice has not yet been used for the investigation of the *HPR1* gene. In order to study the effect of altered HPR1 activities on plant growth, as well as other phenotypes, the annotated rice *OsHPR1* gene, which exists as a single copy in the rice genome (Figure S1), was cloned for constructing overexpression (OE) and RNA interference (RNAi) transgenic lines. Different OE lines and RNAi lines were generated and their HPR1 activities were examined. As shown in Table 1, more than 95% of HPR1 activity was decreased in RNAi lines, which was quite similar to the *Arabidopsis hpr1* mutant (Timm et al. 2008), and almost 50% of HPR1 activity was increased in OE plants. Thus, according to the enzyme activities, two lines, RNAi-1 and OE-1, were chosen for the following experiments. Unsurprisingly, such a pronounced change in HPR1 activity did not have any significant effects on the phenotype of these transgenic plants when compared with WT plant, except a slightly slower growth of RNAi plant grown in normal air (Figure 1A, B). Gene expression of *OsHPR1* was detected in these plants and results showed that mRNA of *HPR1* was hardly found in RNAi plants and roots of WT plants, whereas in OE plants, except a higher expression level of *OsHPR1* gene in leaf than that in WT plants, we also found that *HPR1* mRNA was abundant in the roots of OE plants (Figure 1C). The protein abundance of HPR1 detected by a specific rice HPR1

Table 1. NADH-HPR activity in RNAi and OE lines of *HPR1* gene

Transgenic lines	HPR activity (μmol/min mg protein)	%
WT	1.5781 ± 0.137	/
RNAi-1	0.0589 ± 0.001	−96.27
RNAi-2	0.0806 ± 0.003	−94.89
RNAi-3	0.0778 ± 0.004	−95.07
RNAi-4	0.0674 ± 0.006	−95.73
RNAi-5	0.0688 ± 0.001	−95.64
OE-1	2.2602 ± 0.076*	+43.23
OE-2	1.9557 ± 0.092*	+23.94
OE-3	1.7008 ± 0.162*	+7.78

Mean activities ± *SD* from three measurements per line. Percentage values after comparing with WT plant are shown, (−) means decrease whereas (+) means increase.
*Indicates values that were determined by the *t*-test to be significantly different ($P < 0.05$) from the wild type.

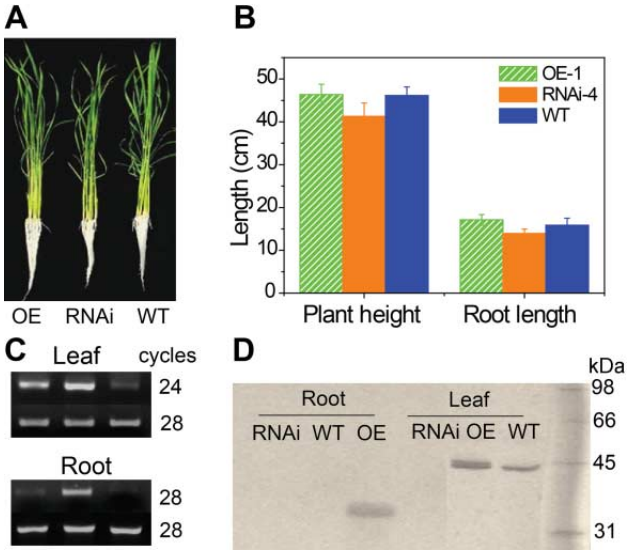

Figure 1. Phenotype of HPR1 RNAi and over expression (OE) plant and expression level of HPR1 gene in these plants
Transgenic plant were constructed as described in Materials and Methods Section, 2-week-old seedlings were used for detection of plant height and root length **(B)**, semiquantitative RT-PCR **(C)**, Western Blot **(D)** of HPR1. Values in **(B)** are means ± *SD* ($n = 30$).

antibody was consistent with its RNA level (Figure 1D). Interestingly, the HPR1 protein in root of the OE plants is about 8 kDa smaller than leaf HPR1, indicating that light-regulated alternative splicing also existed in rice, which could be similar to the pumpkin HPR1 gene (Mano et al. 1999).

Alteration of HPR1 activity has little effect on NADPH-dependent HPR activity and GR activity

Although HPR enzymes have been studied for almost 60 years, many investigators still find the subject quite confusing due to the multiple substrates and another enzyme GR, which can also use the same substrate (Kleczkowski and Randall 1988; Givan and Kleczkowski 1992). To study the effect of altering HPR1 activity on other enzymes, both transgenic plants were used to detect HPR and GR activities using different substrates. As shown in Figure 2, the NADH-dependent HPR (HPR1) activity is mainly abundant in rice leaves but only 15% of leaf HPR1 in the roots. Overexpression of *HPR1* increased 100% of HPR1 activity in leaf. The same activity level can also be found in stem and root of OE plant. Whereas in RNAi plant, only 5% of HPR1 activity left in leaf but more than 50% of WT HPR1 activity in the roots (Figure 2A), indicating other enzymes also contribute to the HPR1 activity, especially in the roots. Then, we examined the NADPH-dependent HPR (HPR2) activity, as shown in Figure 2B, and the highest HPR2 activity is detected in the roots, which is three times of that in leaf. Although a similar pattern was found in transgenic lines, changing HPR1 activity did not affect HPR2 activity significantly, suggesting the HPR2, which differs from HPR1, exists in rice. Similar results were also found in NADH-dependent GR and NADPH-dependent GR (Figure 2C, D). These results suggest that alternative-spliced HPR1 in the root of OE plant as well as GR enzymes do not contribute to HPR2 activity in rice.

Changes of HPR1 alter steady state of metabolite profiles

As the unique mutant that does not have a photorespiration phenotype and resembles WT plant, the *hpr1* mutant has different metabolite profiles, especially in the photorespiration pathway. Hydroxypyruvate (HP) content was quite low in the leaf and even undetectable in the root of WT and OE plants (Figure 3). However, knockout of the rice *HPR1* gene resulted in 45-fold higher HP content than in WT plants. Even the HP content in roots of RNAi plants were detectable, which could be transported from the leaves.

As the substrate of SGAT, which catalyze serine (Ser) and glyoxylate into HP, Ser content was about sixfold higher in leaves of RNAi plant than of that in WT leaves (Figure 3A), which could be responsible for enhanced levels of phospho-serine (P-Ser), which is a precursor of Ser. Glycine (Gly) and glyoxylate accumulated less than Ser did, about 2.5 times and 2 times higher in leaves of RNAi plant, respectively (Figure 3A). In rice root, only Ser accumulated slightly (50%) in *hpr1* RNAi plant,

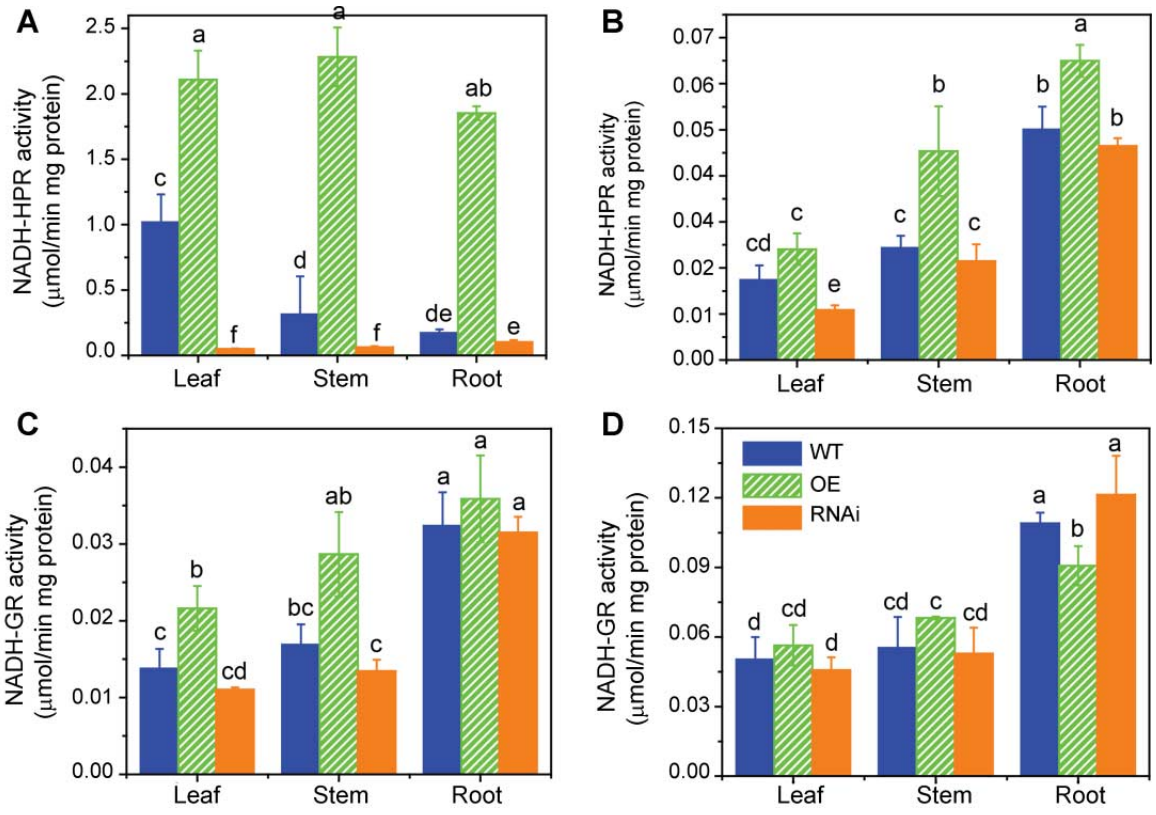

Figure 2. Hydroxypyruvate reductase and Glyoxylate reductase activities in HPR1 overexpression and RNA interference plants
Leaf, stem and root of 2-week-old seedlings were sampled for enzyme assay. **(A)** NADH-HPR (HPR1) activity using HP and NADH as substrate. **(B)** NADPH-HPR (HPR2) activity using HP and NADPH as substrate. (**C**) NADH-GR activity which uses NADH and glyoxylate as substrate. **(D)** NADPH-GR which use NADPH and glyoxylate as substrate. Values are means ± *SD* ($n = 3$). Means denoted by the same letter did not significantly differ at $P < 0.05$ according to Duncan's multiple range test.

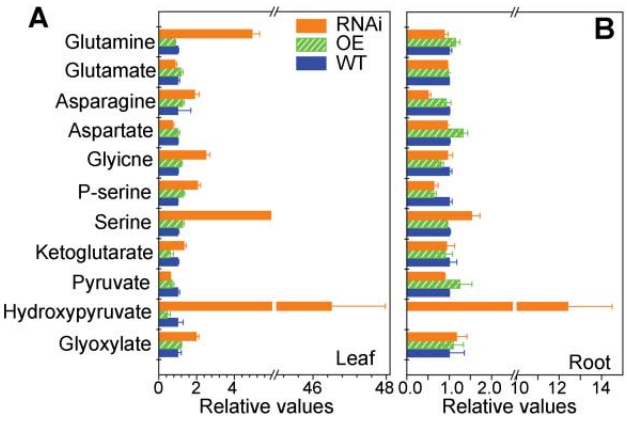

Figure 3. Alteration of the leaf (A) and root (B) content of selected metabolites in the HPR1 overexpression and RNA interference plants

Plants were grown in normal air (380–400 μL/L CO_2), leaves and root of 2-week-old seedlings were sampled for metabolites determination. Mutant/WT and OE/WT ratios of mean metabolite contents ± *SD* ($n = 3$) are shown, where the mean WT values are arbitrarily set to 1.

which is similar to HP (Figure 3B). Glutamate (Glu)-glutamine (Gln) and aspartate (Asp)-asparagine (Asn), both of which play a key role in control in the amino acid content in plants, have a similar accumulation pattern (Figure 3A). Besides, the contents of α-ketoglutarate increased by 32% and decreased by 40% in leaves of RNAi and OE plant, respectively (Figure 3A). These results clearly showed that mutation of *OsHPR1* results in accumulation of intermediates of photorespiration pathway, the accumulation extent of different intermediate depends on its relation to *HPR1* gene. Pyruvate is one of the most important intermediates, which connects different metabolism pathways in plants. Its content was reduced by upregulating or downregulating HPR1 activity (Figure 3A), indicating the metabolism in transgenic plants was disturbed, which was consistent with the observation of the *hpr1* mutant of barley and *Arabidopsis*, in which the photosynthesis and photorespiration were reduced (Murray et al. 1989; Timm et al. 2008). All these results indicate that a cytosolic HPR2 also exists in rice to play a role in the bypass flow of the photorespiration pathway.

Identification of *OsHPR2* in rice

Except *Arabidopsis*, the specific *HPR2* gene has not yet been reported in other plants to date, including rice. In this study, BLASTn was used to search the rice genome according to the sequence of the *AtHPR2* gene (http://rice.plantbiology.msu.edu). Two sequences of the same size (951 bp), Os01g12830.1 and Os01g12830.2, have been found in the rice genome, both of which possess the D-isomer specific 2-hydroxyacid dehydrogenase activity, similar to AtHPR2. Interestingly, these two genes are alternatively spliced from the same gene and share the same 440 bp fragment at the N-terminal (Figure S2, Altschul et al. 1997), which is quite different with *AtHPR2* gene. Thus, these two candidates were used for the following experiments.

It is well known that HPR1 protein is located in the peroxisome, whereas HPR2 belongs to cytosol. However, no evidence about their localization has been reported in rice. In the present study, the subcellular localization of HPR1 and HPR2 protein was first predicted to be located in the peroxisome and cytosol respectively, according to the method of Emanuelsson et al. (2007). Then, both HPR proteins fused to GFP protein were introduced into the protoplast of rice. The CFP fusion with PTS1 signaling peptide and blue spots, which specifically localized in the peroxisome and was used as a control, was observed to be diffused throughout the cytosol in rice protoplasts (Figure 4A). In agreement with the prediction of HPR1 localization, the spots of HPR1-GFP and PTS1-CFP fusions were quite similar in the cotransformation protoplast (Figure 4B–D), indicating the subcellular localization of HPR1 protein is in the peroxisome. By contrast, the fluorescent pattern of chimeric protein with HPR2 was found to accumulate in the cytosol and on the surface of the nucleus (Figure 4E, F). These results provide a solid evidence for the peroxisomal and cytosolic localization of HPR1 and deduced HPR2 protein, respectively.

OsHPR2 knockout plants resemble WT plants grown under air condition

In rice, two *HPR2* candidates have been found using the sequence of *AtHPR2* to blast rice genome. In order to totally knockout the HPR2 activity, the DNA fragment with the same sequence from N-terminal of *OsHPR2-1* and *OsHPR2-2* genes were used for RNA interference (Figure S2). After transformation via agrobacterium, different RNAi lines of *OsHPR2* genes were generated (Figure 5A). All of these lines resemble WT plant in plant height and root length (Figure 5B). RNA analysis by RT-PCR shows that *HPR2-1* and *HPR2-2*, unlike *OsHPR1*, which only expresses in leaves, were abundant in the leaves and roots. Both *OsHPR2* genes were knocked out in lines of RNAi6 and 8 and knocked down in RNAi line 15 (Figure 5C).

Then the enzyme activities were examined in these transgenic plants. As shown in Figure 6, the NADH-HPR (HPR1) activity was dramatically changed in *OsHPR1* overexpression and RNAi lines, whereas mutation of *OsHPR2* genes did not have any significant effect on HPR1 activity in leaf. By contrast, the NADPH-HPR (HPR2) activity was reduced in *OsHPR2* RNAi lines but slightly decreased in *hpr1* mutants both in leaves and roots (Figure 6). Interestingly, the HPR2 activity was exactly consistent with the mRNA level of *OsHPR2* genes (Figure 5C), indicating that proteins encoded by *HPR2* candidates were NADPH-HPR enzyme. Besides, similar to the *OsHPR1* gene, deletion of *OsHPR2* genes did not have any significant effect on NADH-GR and NADPH-GR activities, further indicating that GR enzymes do not contribute to HPR2 activity in rice. These results suggest that the *OsHPR1* gene is responsible for the NADH-HPR activity, whereas *OsHPR2* genes are responsible for the NADPH-HPR activity in rice.

Deletion of *OsHPR2* also perturbs flux of the photorespiration pathway and oxalate content

Although activity of HPR2 is no more than 10% of HPR1 in leaves, it was reported that deletion of HPR2 can also change the metabolite profiles (Timm et al. 2008). In this study, we examined the activity of SGAT, which provides HPRs with substrate in the photorespiratory pathway and thus has a close relationship with HPRs. Our results clearly show that SGAT activity increased in RNAi plants of *OsHPR1* and *OsHPR2* genes

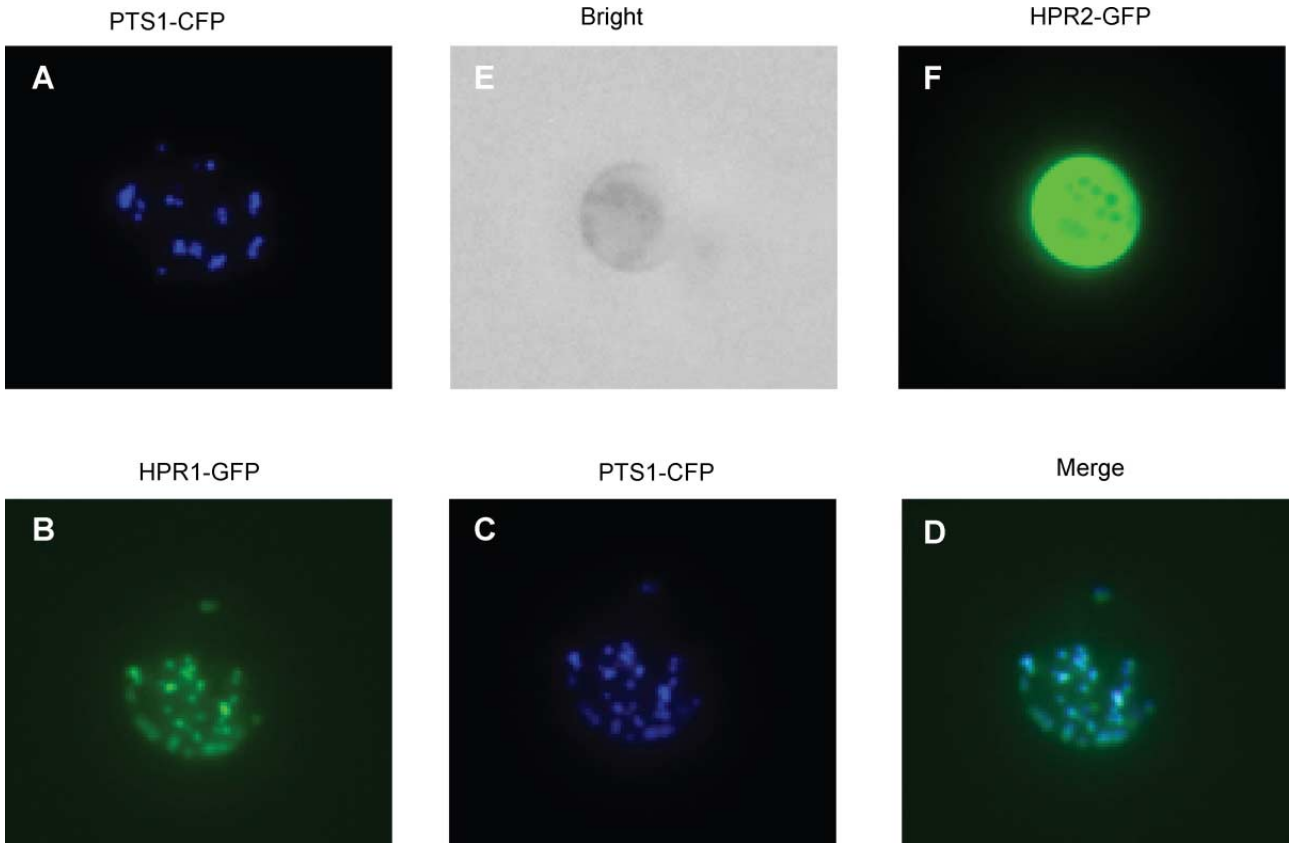

Figure 4. Subcellular localizations of green fluorescent protein (GFP)–HPR1 and GFP-HPR2 fusions in transgenic rice protoplasts
(**A**) Peroxisomal targeting signal fused CFP protein was used as control of peroxisomal localization. (**B**–**D**) Cotransformation of HPR1-GFP and PTS1-CFP fusions to the same protoplast cell, indicating the same localization of HPR1-GFP and PTS1-CFP fusions. (**E**, **F**) light field and blue light excitation (470–490 nm) of HPR2-GFP transformed protoplast.

when compared with WT plant, which could due to the higher content of Ser and Gly in these plants (Figure 3). Interestingly, the SGAT activity also increased in leaves of the OE plant, indicating a rapid photorespiration flow in this plant (Figure 7A). Besides, our previous studies have proved that glyoxylate is an efficient precursor for oxalate in rice (Yu et al. 2010). Because glyoxylate content was increased in *hpr1* RNAi plants, we thus detected the content of oxalate in all transgenic plants. It is shown that oxalate contents are increased in *hpr1* RNAi plants and *hpr2* RNAi plants, except overexpression plants (Figure 7B) because glyoxylate content in this OE plant is similar to that in WT plants. These results indicate that cytosolic HPR2 is an efficient compensation for the peroxisomal HPR1 function and plays an important role in photorespiration pathway in rice.

Double deletion of *OsHPR1* and *OsHPR2* genes significantly reduces plant growth under normal photorespiration condition

To further prove that *OsHPR2* is an efficient compensation for *OsHPR1*, a double deletion of *OsHPR1* and *OsHPR2* genes was performed for this study. By crossing the *hpr1* and *hpr2* mutants, we generated the double mutant of *hpr1* × *hpr2*. Homozygote of the double mutant was used for the phenotype compared with WT plant. As shown in Figure 8, when plants were grown under atmospheric conditions, the double mutation of *OsHPR1* and *OsHPR2* displayed a significant retardance, although mutants of *hpr1* and *hpr2* resemble WT plant. However, when these mutants were grown in elevated CO_2 (0.5%), the plant growth was similar with WT plant, which is a typical photorespiration phenotype (Figure 8B). These results strongly prove that the HPR2 protein of this study is the cytosolic HPR, which can efficiently compensate for the function of peroxisomal HPR1 in photorespiration of rice.

DISCUSSION

In higher plants, photorespiration will cut down up to 25% CO_2 assimilation, indicating a substantial carbon flux in the photorespiration cycle (Timm et al. 2012). Thus any mutation that can interrupt this flow will result in a lethal phenotype (Somerville 2001; Timm and Bauwe 2012). However, an exception is the mutant *HPR1* gene is not lethal but only slightly sensitive to atmosphere air (Murray *et al.* 1989; Timm et al. 2008). HPR1 is one of the most active enzymes in the C2 cycle and thus is not a limited-step of this pathway. This extremely high activity of HPR1 leads to a very low level of HP content in the leaves of WT plants under air conditions (Figure 3A). Interestingly, although *hpr1* mutants resemble WT

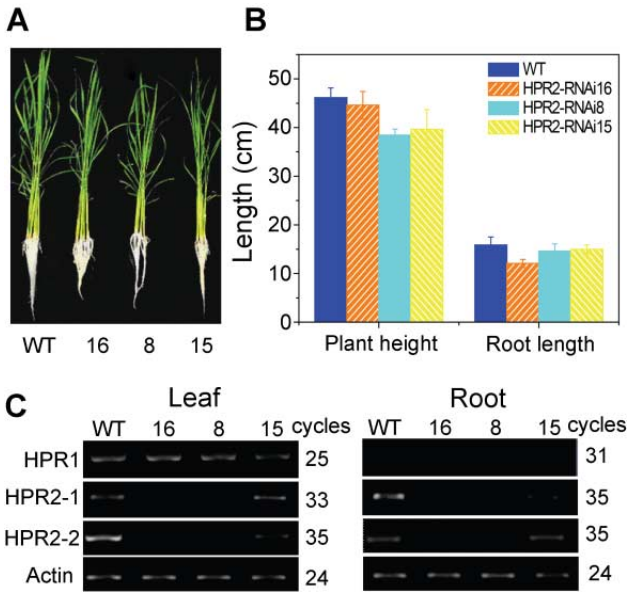

Figure 5. Phenotype of HPR2 RNAi plants and expression level of HPR genes in these plants
Transgenic plants were constructed as described in Materials and Methods, numbers in **(A)** stand for line name of HPR2 transgenic lines. Two-week-old seedlings were used for detection of plant height and root length **(B)**, semiquantitative RT–PCR of HPR1 **(C)**. Values in **(B)** are means ± *SD* ($n = 30$).

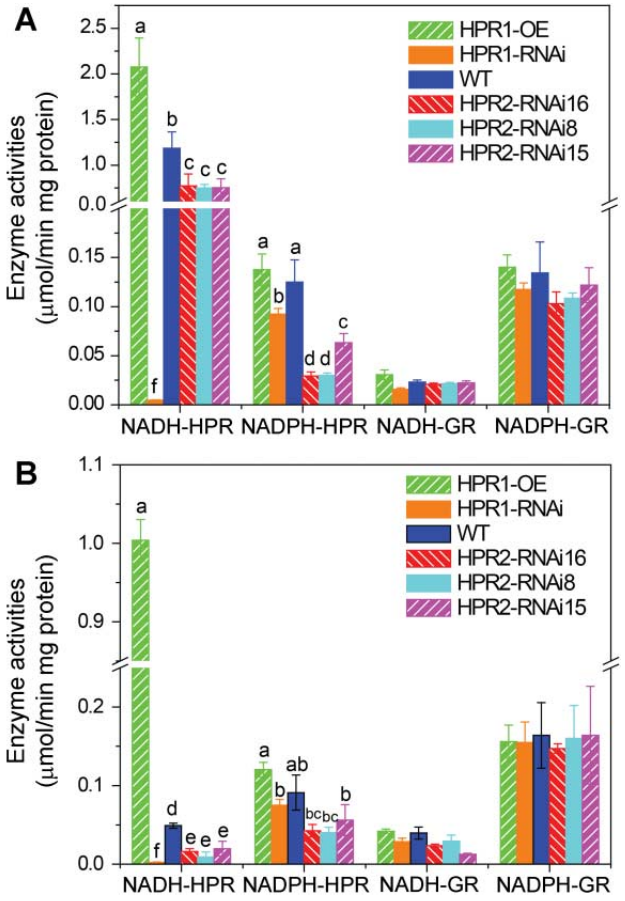

Figure 6. Hydroxypyruvate reductase and Glyoxylate reductase activities in HPR1 overexpression, HPR1 RNA interference and HPR2 RNA interference plants. Leaf and root of 2-week-old seedlings were sampled for enzyme assay
(A) HPR activities and GR activities in leaves of all transgenic lines in this study. **(B)** HPR activities and GR activities in roots of all transgenic lines in this study. Values are means ± *SD* ($n = 3$). Means denoted by the same letter did not significantly differ at $P < 0.05$ according to Duncan's multiple range test, compares were performed in the same enzymes and only the HPRs were shown.

plant, the HP and Ser content actually increased significantly in this mutant, especially the HP content (Figures 1, 3). Although accumulation of HP and Ser is not harmful to plant, it has been recently reported that accumulation of Ser can deregulate photorespiration-related gene expressions (Timm et al. 2013). Thus, in this *hpr1* mutant, there must be a bypass that effectively compensates for the loss of HPR1 function and keeps the photorespiratory flow going, because photorespiratory flux is only slightly slowed down in this mutant by the accumulated serine in a feedback mechanism.

Ever since its identification, the *hpr1* mutant has been well-known for its distinctive feature of viability in atmosphere air when compared with other mutants in the photorespiration pathway. The expression pattern of the *OsHPR1* gene has been intensively investigated to find out the compensation bypass for deficiency of this unique gene (Kleczkowski et al. 1990; Jin et al. 1998; Mano et al. 2000). Studies in pumpkin and cucumber have revealed that expression of *HPR1* gene is light inducible. Especially in pumpkin, light regulates the alternative splicing of pre-mRNA of *HPR1* to produce two localized-HPR proteins, the peroxisomal HPR1 and cytosolic HPR2 (Jin et al. 1998; Mano et al. 1999). In rice, HPR1 protein cannot be found in the roots of WT plants. However, in roots of OE plants, the HPR1 activity is extremely high (Figure 2A) and, interestingly, in a smaller form compared with HPR1 in leaves (Figure 1C). It seems that rice can also produce HPR2 by alternative splicing in the roots but not in leaf. However, HPR2 purified in spinach leaf differs with HPR1 in molecular weight, K_m value for hydroxypyruvate and prefers NADPH to NADH as cofactor (Kleczkowski and Randall 1988). Furthermore, barley *hpr1* mutant shows a similar HPR2 activity with WT plant (Kleczkowski et al. 1990; Igamberdiev and Kleczkowski 2000). These investigations strongly prove that HPR2 is encoded by a new gene that differs with the peroxisomal HPR1 gene. Similar to their results, HPR1 activity was downregulated by 95% in leaves of RNAi plants of this study, but resembling WT plants in phenotype and with little effect on HPR2 activity (Figure 2). This is in agreement with the hypothesis that a cytosolic NADPH-HPR will compensate for the HPR1 function. The identification of *AtHPR2* in *Arabidopsis* was the first time to clone the *HPR2* gene, which was not alternatively spliced from HPR1 DNA and thus proved the bypass hypothesis (Timm et al. 2008). However, another question whether more than one mechanism for photorespiratory bypass exists in different species has arisen, which is the primary concern in this study.

For a better understanding of the photorespiration pathway in rice, we have constructed a *hpr1* RNAi mutant, which was then used for identification of *OsHPR2* in rice. In this

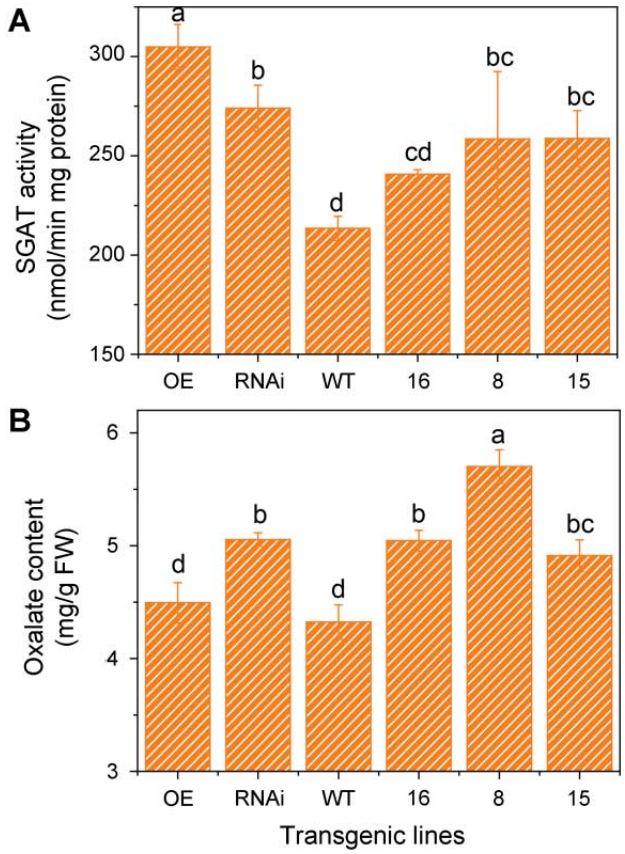

Figure 7. Serine glyoxylate aminotransferase (SGAT) activity (A) and Oxalate content (B) in leaves of HPR1 over expression, HPR1 RNA interference, and HPR2 RNA interference plants
Leaves of 2-week-old seedlings were sampled for enzyme assay oxalate determination. Values are means ± *SD* ($n = 3$). Means denoted by the same letter did not significantly differ at $P < 0.05$ according to Duncan's multiple range test.

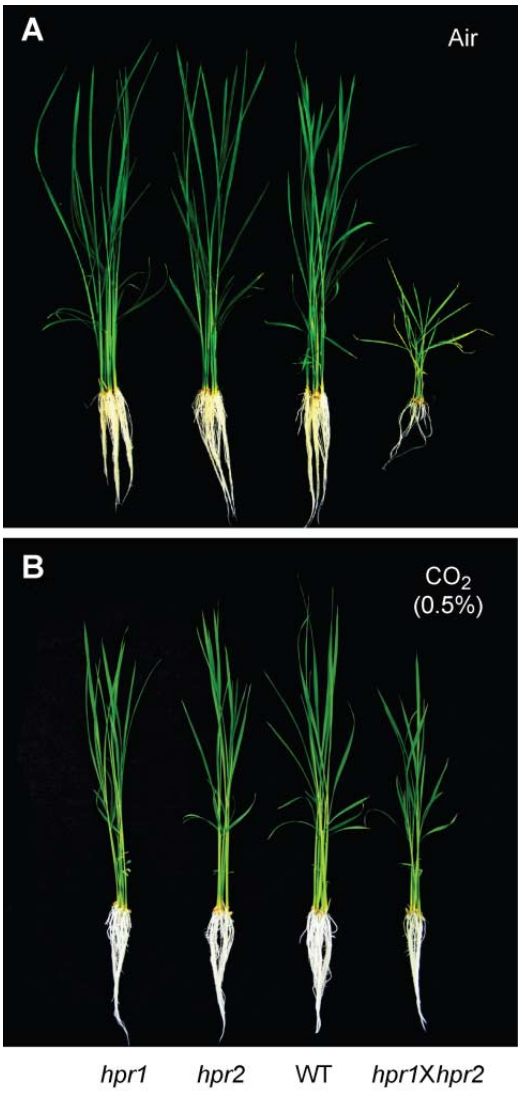

Figure 8. The individual interference of either *HPR1* or *HPR2* is well tolerated in normal air, but combined deletion causes significantly air sensitivity
(A) Individual mutant of *hpr1* and *hpr2* and double mutant of *hpr1* × *hpr2* were grown under normal air condition, compared with wild type (WT) plant. **(B)** WT plant, individual mutant of *hpr1* and *hpr2* and double mutant of *hpr1* × *hpr2* were grown in elevated CO_2 (0.5%) condition.

study, two mRNAs were found to be the *OsHPR2* gene according to the sequence of *AtHPR2* gene. Further alignment analysis revealed that these two mRNAs were alternatively spliced from the same gene. RNA interference vector using the same fragments in these two mRNAs was then transformed into WT plants. Fortunately, different RNAi lines display a significant decrease of NADPH-dependent HPR activity without any effect on NADH-dependent HPR activity (Figure 6), although the phenotype of these transgenic plants resembles WT plant (Figure 5). Both enzyme activities and phenotypes appear like other *hpr1* mutants in barley and *Arabidopsis* (Murray et al. 1989; Timm et al. 2008). These results indicated that the rice *OsHPR2* gene has been tentatively identified in the present study.

Many proteins in the peroxisome possess a unique signaling peptide at their C terminals, which is called peroxisomal targeting signal 1 (PTS1), including the HPR1 protein (Gould et al. 1987, 1989; Greenler and Becker 1990). Without this targeting peptide, proteins cannot locate to the peroxisome, such as HPR2 of pumpkin and *Arabidopsis*, both of which are predicted to locate to cytosol, although no direct evidence has been shown in that research (Mano et al. 1999; Timm et al. 2008). In the present study, our transient expression results clearly proved that without PTS1 targeting signal, HPR2 could not be sorted into peroxisome but stayed in cytosol (Figure 4), indicating the HPR2 played a compensation role in cytosol by catalyzing HP leaked from peroxisome into glycerate. Mutation of *OsHPR1* did not change the phenotype of mutant plants when compared with WT plants. However, it did disturb the carbon flux of the photorespiratory pathway (Figure 3). Besides, content of oxalates increased significantly owing to the accumulated content of glyoxylate in *hpr1* RNAi plants (Yu et al. 2010). Similar to these results, the oxalate content and SGAT activity, which provides HPR with substrate in the photorespiration pathway, were both increased in *hpr2*

RNAi plants (Figure 7A). Although *in vitro* activity of HPR2 is much lower than that of HPR1, individual mutants of both genes display a similar effect on photorespiration flux in rice. Besides, the *Arabidopsis* double mutant of both peroxisomal malate dehydrogenase isoforms (PMDH), which provide HPR1 with NADH, was reported to be viable in normal air conditions with slightly impaired photosynthetic rates when compared with WT plants, resembling *hpr1* mutant (Cousins et al. 2008). Results obtained from different plants obviously proved that HPR2 is somewhat important in catalyzing HP into glycerate in plants even under normal conditions.

Except the HPR enzymes, there are still some other enzymes that can use HP as a substrate, such as the glyoxylate reductases in spinach (Kleczkowski et al. 1986), and lactate dehydrogenase in *Arabidopsis* (Betsche 1981). However, their contributions to photorespiration flux were not examined. Double mutants of *hpr1* and *hpr2* of *Arabidopsis* is not lethal but grow slowly because of the *AtHPR3* in the chloroplast (Timm et al. 2011). Growth retardance in double mutant *hpr1* and *hpr2* is much more significant than another double mutant *hpr1* and *hpr3* of *Arabidopsis*, which is similar to the single mutant of *hpr1*, suggesting that HPR1, together with HPR2, are predominant enzymes that converting HP into glycerate. In our study, a double mutant of *hpr1* and *hpr2* of rice, generated by crossing the corresponding RNAi lines, was dramatically retarded in growth under normal air conditions. However, when this plant was grown in elevated CO_2 (0.5%), it displayed a similar phenotype to WT plants (Figure 8), which is a typical photorespiratory phenotype. These results provide solid evidence that rice NADPH-HPR is encoded by the *OsHPR2* gene rather than by light-induced alternative splicing from the *OsHPR1* gene and that both HPR enzymes are involved in photorespiratory metabolism in rice.

MATERIALS AND METHODS

Plant material and growth conditions

Rice seeds (*Oryza sativa* L. cv. Zhonghua 11) were surface sterilized by NaClO for 20 min and soaked in distilled water overnight, and then germinated in a Petri dish with filter papers in darkness at 28 °C for 2–3 d until the root measured 1 cm. Germinated seedlings were transferred to a black mesh and grown in Kimura B nutrient solution with a renewal every 3 d. Unless otherwise stated, plants were grown in normal air (380–400 μL/L CO_2) and in air with elevated CO_2 (0.5%) in controlled-environment chambers (Conviron, Manitoba, Canada) with a day/night cycle of 14/10 h (28 °C/25 °C, approximately 400 μmol/m^2 s irradiance). Samples of rice leaves from different plants were stored at −80 °C for intermediate determination, enzyme assays, and RNA isolation. Triplicates were set for all the experiments.

Construction of transgenic lines and plasmids for transient expression and prokaryotic expression

Rice (*Oryza sativa* L. cv. Zhonghua 11) was used for over-expression and RNA interference transformations in this study. The OE and RNAi vector pYL was kindly provided by Dr Yao-Guang Liu (South China Agricultural University, Guangzhou). To generate the pYL-HPR1 overexpression construct, the complete cDNA of *OsHPR1* (NM_001052124) was cloned by reverse transcription-polymerase chain reaction (RT-PCR), and then inserted into pYL between *Hin*dIII and *Mul*I restriction sites. To generate RNA interference lines, the selected fragments from target genes were first cloned into pYL, and then the inverse DNA fragments were amplified by a special primer from the pYL vector and cloned into the same vector used for amplification. All the constructs were transformed into rice callus by Agrobacterium-mediated infection (strain EHA105). After hygromycin selection, T0 transgenic plants were regenerated, which was followed by a PCR check of the hygromycin phosphotransferase marker gene. Then the southern blot and HPR enzyme activities were used for generating the T2 homozygous plants of *HPR1* and *HPR2* genes.

Plasmids for transient expression and prokaryotic expression were also constructed. The selected DNA fragments were cloned into pHPR1-GFP, pHPR2-GFP, and pET-30a vectors, respectively. All the primers used in this study are shown in Table S1.

Preparation of HPR1 antibody and Western blot analysis

The antibody was prepared by expressing the complete *OsHPR1* cDNA (inserted into a pET-30a vector; Novagen, Darmstadt, Germany) in *Escherichia coli* (BL21). The expressed HPR1 protein induced by isopropyl-b-D-thiogalactopyranoside was purified on 4–20% gradient sodium dodecyl sulfate–polyacrylamide gel electrophoresis (SDS–PAGE) and then injected into a rabbit. The serum was withdrawn as the antibody.

Proteins were extracted by homogenizing 0.2 g fresh leaves in 4 mL 20 mM phosphate buffer (pH 8.0). The homogenate was centrifuged at 18 000 *g* or 15 min. Equally loaded proteins (50 μg) were separated by 12% SDS–PAGE, then transferred to a nitrocellulose membrane. The membrane was blocked for 60 min with 5% (w/v) nonfat milk in 0.05% (w/v) Tween 20, 10 mM Tris (pH 8.0) and 150 mM NaCl. The antibody was added and incubated at 4 °C overnight. After washing, the alkaline horseradish peroxidase (HRP)-coupled secondary antibody was added and incubated at room temperature for 1.5 h. The color was developed with a solution containing H_2O_2.

RNA isolation and Semiquantitative PCR analysis of gene expressions

Total RNA was extracted from rice seeds with a Plant RNA Isolation Mini Kit (Agilent Technologies, Santa Clara, CA, USA) and then digested with RNase-free DNase I (Amersham, Piscataway, NJ, USA) to eliminate genomic DNA contamination. First-strand cDNA was synthesized with oligo(dT) primers using a SuperScript first-strand synthesis system according to the manufacturer's instructions (Invitrogen, Grand Island, NY, USA). Transcript levels of each gene were measured by Semiquantitative PCR. The optimal number of PCR cycles was first tested gene by gene during semiquantitative PCR analysis. The PCR was performed with PTC-200 (Bio-Rad, Hercules, CA, USA), and the PCR products were separated on 1% (w/v) agarose gels and visualized by Goldview staining. Sequences of the primers for the semiquantitative RT-PCR were listed in Table S1.

Assay of enzyme activities

SGAT

One hundred milligrams of leaves were homogenized in 1 mL 50 mM K-phosphate (pH 7.4) at 4 °C, and the homogenate was then centrifuged at 15 000 *g* and 4 °C for 30 min. The supernatant was used as an enzyme extract. The reaction mixture (500 μL) contained 20 mM L-serine for SGAT, 5 mM

glyoxylate, 10 μM pyridoxal-5-phosphate (PAL), and appropriate enzyme extract. The reaction was started by the addition of glyoxylate and conducted at 30 °C for 20 min. The reaction was terminated by adding 100 μL of 20% trichloroacetic acid (TCA). After a centrifugation, the supernatant was derived with dinitroflurobenzene at 60 °C for 1 h. The amino acid derivatives were then separated on a C-18 column equipped with a high performance liquid chromatography (HPLC) system (Waters Corporation, Milford, MA, USA) and the amount of glycine produced was detected to measure the SGAT activity.

HPR and GR activities

One hundred milligrams of leaves were homogenized in a 1 mL extraction buffer (10 mM Tris–HCl, 1 mM ethylenediaminetetraacetic acid (EDTA), 2 mM $MgCl_2$, and 1 mM β-mercaptoethanol, pH 7.5) at 4 °C, then the homogenate was centrifuged at 15 000 *g* and 4 °C for 20 min. The supernatant was used for HPR and GR activity assays. One milliliter of reaction mixture contained the extraction buffer as described above, 0.2 mM NADH or NADPH, 0.5 mM hydroxypyruvate for HPR, or 1 mM glyoxylate for GR, and the appropriate enzyme extract. The reaction was started by the addition of hydroxpyruvate or glyoxylate, and the oxidation of NADH or NADPH was spectrophotometrically detected at 340 nm. Protein concentrations were determined according to Bradford (1976), using BSA as a standard.

Extraction and quantification of organic acids and free amino acids

Oxalate and other organic acids and free amino acids were determined according to Xu et al. (2006, 2009) with slight modifications. Rice samples of leaf and root (0.1 g) were harvested and immediately frozen in liquid N_2 then stored at −80 °C for subsequent measurements. The samples were homogenized in 1 mL of 0.5 N HCl. The homogenate was heated at 80 °C for 10 min with intermittent shaking. Distilled water was added to the homogenate to a volume of 5 mL. One milliliter of the diluted homogenate was withdrawn and centrifuged at 15,000 *g* for 10 min. Then 0.5 mL of the supernatant was filtered through a 0.45 μm membrane. For high-performance liquid chromatography (HPLC) analysis, different organic acids in the filtrate were first derivatized by phenylhydrazine to form phenylhydrazone. The derivative was separated and quantified by reversed phase HPLC analysis with an Alliance 2695 reversed-phase system (Waters, Wexford, Ireland), and a Waters 2487 UV detector set at 324 nm. Ten microliters of each sample were injected into a reversed-phase column (Sun Fire, C18 column, 5 μm, 4.6 mm × 250 mm; Waters). The mobile phase consisted of 5% methanol and 95% phosphate buffer (13 mM potassium biphosphate; 1 mM potassium phosphate dibasic, pH 6.0). Analytes were quantified from the ratio of their respective peak areas to the peak area of the standard curve.

Free amino acids were determined according to Masclaux-Daubresse et al. (2006). The rice leaf and root were sampled as described above at 0.2 g each. First, three replicate samples were pooled together (total 0.6 g) and homogenized in 3 mL of 4% (w/v) sulfosalicylic acid. The homogenate was kept at room temperature for 2 h, then centrifuged at 21 000 *g* for 20 min. Free amino acids in the supernatant were analyzed by a high-speed automatic amino acid analyzer (Hitachi 835-50; Tokyo, Japan).

Protoplast isolation and transient expression

Transient expression experiments were performed according to Chen et al. (2006). For isolating protoplasts from young seedling tissues, rice seeds were germinated on half-strength MS medium under light for 3 d. Seedlings were then cultured on half-strength MS medium in the dark at 26 °C for 10–12 d. Tissues of etiolated young seedlings were cut into approximately 0.5 mm strips and placed in a dish containing K3 medium supplemented with 0.4 m sucrose, 1.5% cellulase R-10 (Yakult Honsa) and 0.3% macerozyme R-10 (Yakult Honsha). The chopped tissue was vacuum-infiltrated for 1 h at 20 mmHg and digested at 25 °C with gentle shaking at 40 rpm. After incubation, the K3 enzyme medium was replaced by the same volume of W5 solution (154 mM NaCl, 125 mM $CaCl_2$, 5 mM KCl, and 2 mM MES, adjusted to pH 5.8 with KOH). Protoplasts were released by shaking at 80 rpm for 1 h, followed by filtering through a 35 μm nylon mesh. Protoplasts were collected by centrifuging at 300 *g* for 4 min at 4 °C. Pellets were resuspended in W5 solution. The leaves and the stems including sheaths were used to compare protoplast yields with a 12 h digestion time.

The collected protoplasts were resuspended in an appropriate volume of suspension medium (0.4 m mannitol, 20 mM $CaCl_2$, and 5 mM MES, adjusted to pH 5.7 with KOH). Plasmid DNAs (about 10 μg DNA of each construct) were mixed with 200 μL of suspended protoplasts (usually 1.5–2.5 × 10^6 cells/mL). The DNA and protoplasts mixture was added to 40% polyethylene glycol (PEG) solution (40% PEG 4000, 0.4 M mannitol and 100 mM $Ca(NO_3)_2$, adjusted to pH 7.0 with 1 M KOH) and mixed immediately by gently shaking, and then incubated for 20 min at room temperature. After incubation, 1.0 mL W5 medium was added to the tube to dilute PEG. For the experiments designed for fluorescence microscopy, the K3 medium was used instead of the W5 medium.

Fluorescence microscopy was performed under a Nikon Eclipse E600 fluorescence microscope (Nikon, Tokyo, Japan). Excitation and emission filter Ex450–490/DM510/BA520-560 were used for GFP, respectively. Images were captured with a SPOT 2 Slider charge-coupled device camera.

ACKNOWLEDGEMENTS

We are grateful to Professor Yaoguang Liu (College of Science, South China Agricultural University) for providing us with the pYL vector. This work was supported by the National Natural Science Foundation of China (U1201212; 31170222), the Shenzhen Overseas Talents Innovation and Entrepreneurship Funding Scheme (The Peacock Scheme) and China Postdoctoral Science Foundation (2013M530374).

REFERENCES

Altschul SF, Madden TL, Schäffer AA, Zhang J, Zhang Z, Miller W, Lipman DJ (1997) Gapped BLAST and PSI-BLAST: A new generation of protein database search programs. **Nucleic Acids Res** 25: 3389–3402

Bauwe H, Hagemann M, Fernie AR (2010) Photorespiration: Players, partners and origin. **Trends Plant Sci** 15: 330–336

Bauwe H, Hagemann M, Kern R, Timm S (2012) Photorespiration has a dual origin and manifold links to central metabolism. **Curr Opin Plant Biol** 15: 269–275

Betsche T (1981) L-Lactate dehydrogenase from leaves of higher plants. Kinetics and regulation of the enzyme from lettuce (*Lactuca sativa* L.). **Biochem J** 195: 615–622

Boldt R, Edner C, Kolukisaoglu Ü, Hagemann M, Weckwerth W, Wienkoop S, Morgenthal K, Bauwe H (2005) D-Glycerate 3-kinase, the last unknown enzyme in the photorespiratory cycle in *Arabidopsis*, belongs to a novel kinase family. **Plant Cell** 17: 2413–2420

Bradford MM (1976) A rapid and sensitive method for the quantitation of microgram quantities of protein utilizing the principle of protein dye binding. **Anal Biochem** 72: 248–254

Chen S, Tao L, Zeng L, Vega-Ssanchez ME, Umemura K, Wang GL (2006) A highly efficient transient protoplast system for analyzing defence gene expression and protein–protein interactions in rice. **Mol Plant Pathol** 7: 417–427

Cousins AB, Pracharoenwattana I, Zhou W, Smith SM, Badger MR (2008) Peroxisomal malate dehydrogenase is not essential for photorespiration in *Arabidopsis* but its absence causes an increase in the stoichiometry of photorespiratory CO_2 release. **Plant Physiol** 148: 786–795

Desai M, Hu J (2008) Light induces peroxisome proliferation in *Arabidopsis* seedlings through the photoreceptor phytochrome A, the transcription factor HY5 HOMOLOG, and the peroxisomal protein PEROXIN11b. **Plant Physiol** 146: 1117–1127

Emanuelsson O, Brunak S, von Heijne G, Nielsen H (2007) Locating proteins in the cell using TargetP, SignalP and related tools. **Nat Protoc** 2: 953–971

Florian A, Araújo WL, Fernie AR (2013) New insights into photorespiration obtained from metabolomics. **Plant Biol** 15: 656–666

Givan CV, Kleczkowski LA (1992) The enzymatic reduction of glyoxylate and hydroxypyruvate in leaves of higher plants. **Plant Physiol** 100: 552–556

Gould SJ, Keller GA, Hosken N, Wilkinson J, Subramani S (1989) A conserved tripeptide sorts proteins to peroxisomes. **J Cell Biol** 108: 1657–1664

Gould SJ, Keller GA, Subramani S (1987) Identification of a peroxisomal targeting signal at the carboxy terminus of firefly luciferase. **J Cell Biol** 105: 2923–2931

Greenler JM, Becker WM (1990) Organ specificity and light regulation of NADH-dependent hydroxypyruvate reductase transcriptabundance. **Plant Physiol** 94: 1484–1487

Greenler JM, Sloan JS, Schwartz BW, Becker WM (1989) Isolation, characterization and sequence analysis of a full-length cDNA clone encoding NADH-dependent hydroxypyruvate reductase from cucumber. **Plant Mol Biol** 13: 139–150

Hayashi M, Tsugeki R, Kondo M, Mori H, Nishimura M (1996) Pumpkin hydroxypyruvate reductases with and without a putative C-terminal signal for targeting to microbodies may be produced by alternative splicing. **Plant Mol Biol** 30: 183–189

Hondred D, Wadle DM, Titus DE, Becker WM (1987) Light-stimulated accumulation of the peroxisomal enzymes hydroxypyruvate reductase and serine: Glyoxylate aminotransferase and their translatable mRNAs in cotyledons of cucumber seedlings. **Plant Mol Biol** 9: 259–275

Igamberdiev AU, Kleczkowski LA (2000) Capacity for NADPH/NADP turnover in the cytosol of barley seed endosperm: The role of NADPH-dependent hydroxypyruvate reductase. **Plant Physiol Biochem** 38: 747–753

Jin G, Davey MC, Ertl JR, Chen R, Yu ZT, Daniel SG, Becker WM, Chen CM (1998) Interaction of DNA-binding proteins with the 5′-flanking region of a cytokinin-responsive cucumber hydroxypyruvate reductase gene. **Plant Mol Biol** 38: 713–723

Kleczkowski LA, Edwards GE, Blackwell RD, Lea PJ, Givan CV (1990) Enzymology of the reduction of hydroxypyruvate and glyoxylate in a mutant of barley lacking peroxisomal hydroxypyruvate reductase. **Plant Physiol** 94: 819–825

Kleczkowski LA, Randall DD (1988) Purification and characterization of a novel NADPH (NADH)-dependent hydroxypyruvate reductase from spinach leaves. Comparison of immunological properties of leaf hydroxypyruvate reductases. **Biochem J** 250: 145

Kleczkowski LA, Randall DD, Blevins DG (1986) Purification and characterization of a novel NADPH(NADH)-dependent glyoxylate reductase from spinach leaves. Comparison of immunological properties of leaf glyoxylate reductase and hydroxypyruvate reductase. **Biochem J** 239: 653–659

Mano S, Hayashi M, Kondo M, Nishimura M (1997) Hydroxypyruvate reductase with a carboxy-terminal targeting signal to microbodies is expressed in *Arabidopsis*. **Plant Cell Physiol** 38: 449–455

Mano S, Hayashi M, Nishimura M (1999) Light regulates alternative splicing of hydroxypyruvate reductase in pumpkin. **Plant J** 17: 309–320

Mano S, Hayashi M, Nishimura M (2000) A leaf-peroxisomal protein, hydroxypyruvate reductase, is produced by light-regulated alternative splicing. **Cell Biochem Biophys** 32: 147–154

Masclaux-Daubresse C, Reisdorf-Cren M, Pageau K, Lelandais M, Grandjean O, Kronenberger J, Valadier MH, Feraud M, Jouglet T, Suzuki A (2006) Glutamine synthetase-glutamate synthase pathway and glutamate dehydrogenase play distinct roles in the sink-source nitrogen cycle in tobacco. **Plant Physiol** 140: 444–456

Murray AJ, Blackwell RD, Lea PJ (1989) Metabolism of hydroxypyruvate in a mutant of barley lacking NADH-dependent hydroxypyruvate reductase, an important photorespiratory enzyme activity. **Plant Physiol** 91: 395–400

Peterhansel C, Krause K, Braun HP, Espie GS, Fernie AR, Hanson DT, Keech O, Maurino VG, Mielewczik M, Sage RF (2012) Engineering photorespiration: Current state and future possibilities. **Plant Biol** 15: 754–758

Schwarte S, Bauwe H (2007) Identification of the photorespiratory 2-phosphoglycolate phosphatase, PGLP1, in *Arabidopsis*. **Plant Physiol** 144: 1580–1586

Skadsen RW, Scandalios JG (1987) Translational control of photoinduced expression of the Cat2 catalase gene during leaf development in maize. **Proc Natl Acad Sci USA** 84: 2785–2789

Sloan JS, Schwartz BW, Becker WM (1993) Promoter analysis of a light-regulated gene encoding hydroxypyruvate reductase, an enzyme of the photorespiratory glycolate pathway. **Plant J** 3: 867–874

Somerville CR (2001) An early *Arabidopsis* demonstration. Resolving a few issues concerning photorespiration. **Plant Physiol** 125: 20–24

Somerville CR, Ogren WL (1980) Photorespiration mutants of *Arabidopsis thaliana* deficient in serine-glyoxylate aminotransferase activity. **Proc Natl Acad Sci USA** 77: 2684–2687

Somerville CR, Ogren WL (1981) Photorespiration-deficient mutants of *Arabidopsis thaliana* lacking mitochondrial serine transhydroxymethylase activity. **Plant Physiol** 67: 666–671

Timm S, Bauwe H (2012) The variety of photorespiratory phenotypes—Employing the current status for future research directions on photorespiration. **Plant Biol** 15: 737–747

Timm S, Florian A, Jahnke K, Nunes-Nesi A, Fernie AR, Bauwe H (2011) The hydroxypyruvate-reducing system in *Arabidopsis*: Multiple enzymes for the same end. **Plant Physiol** 155: 694–705

Timm S, Florian A, Wittmiß M, Jahnke K, Hagemann M, Fernie A, Bauwe H (2013) Serine acts as metabolic signal for the transcriptional control of photorespiration-related genes in *Arabidopsis thaliana*. **Plant Physiol** 162: 379–389

Timm S, Mielewczik M, Florian A, Frankenbach S, Dreissen A, Hocken N, Fernie AR, Walter A, Bauwe H (2012) High-to-low CO_2 acclimation reveals plasticity of the photorespiratory pathway and indicates regulatory links to cellular metabolism of *Arabidopsis*. **PLoS ONE** 7: e42809

Timm S, Nunes-Nesi A, Pärnik T, Morgenthal K, Wienkoop S, Keerberg O, Weckwerth W, Kleczkowski LA, Fernie AR, Bauwe H (2008) A cytosolic pathway for the conversion of hydroxypyruvate to glycerate during photorespiration in *Arabidopsis*. **Plant Cell** 20: 2848–2859

Voll LM, Jamai A, Renne P, Voll H, McClung CR, Weber APM (2006) The photorespiratory *Arabidopsis* shm1 mutant is deficient in SHM1. **Plant Physiol** 140: 59–66

Xu H, Zhang J, Zeng J, Jiang L, Liu E, Peng C, He Z, Peng X (2009) Inducible antisense suppression of glycolate oxidase reveals its strong regulation over photosynthesis in rice. **J Exp Bot** 60: 1799–1809

Xu HW, Ji XM, He ZH, Shi WP, Zhu GH, Niu JK, Li BS, Peng XX (2006) Oxalate accumulation and regulation is independent of glycolate oxidase in rice leaves. **J Exp Bot** 57: 1899–1908

Yu L, Jiang J, Zhang C, Jiang L, Ye N, Lu Y, Yang G, Liu E, Peng C, He Z, Peng X (2010) Glyoxylate rather than ascorbate is an efficient precursor for oxalate biosynthesis in rice. **J Exp Bot** 61: 1625–1634

Zelitch I, Day PR (1973) The effect on net photosynthesis of pedigree selection for low and high rates of photorespiration in tobacco. **Plant Physiol** 52: 33–37

SUPPORTING INFORMATION

Additional supporting information may be found in the online version of this article:

Table S1. Primers used for polymerase chain reaction (PCR) amplification of cDNAs and SemiQRT-PCR experiments

Figure S1. Hybridization of *HPR*1 cDNA to endonuclease-digested rice leaf DNA

Figure S2. Sequence Alignment of *HPR*2-1 and *HPR*2-2 genes